Journal of Thermal Analysis and Calorimetry, Vol. 88 (2007) 2, 537–548

METASTABLE EFFECTS ON MARTENSITIC TRANSFORMATION IN SMA Part 4. Thermomechanical properties of CuAlBe and NiTi observations for dampers in family houses

C. Auguet[1,2], *A. Isalgué*[1], *F. C. Lovey*[3], *F. Martorell*[1] *and V. Torra*[1*]

[1]CIRG, DFA, ETSECCPB, UPC, Campus Nord B4, 08034 Barcelona, Catalonia, Spain
[2]DFA, EPSEB, UPC, Av. Dr. Marañón 44, 08028 Barcelona, Catalonia, Spain
[3]Centro Atómico Bariloche and Instituto Balseiro, 8400 S.C. de Bariloche, Argentina

The behavior of shape memory alloys (SMA) allows their use as a passive smart material. In particular, the existence of a hysteretic cycle in the domain of the elementary coordinates strain-stress-temperature (σ, ε, T) suggests its application for damping in mechanical and/or in civil engineering. We are working in the application of SMA as dampers for earthquakes in small houses as family homes. For dampers installed in the inner porticos of the house, the suggested SMA is the CuAlBe and, eventually, the NiTi. At room temperature the used SMA wires induces forces situated between 2–3kN/wire. The properties related with the damping applications for CuAlBe and NiTi, i.e., the SMA creep and the self-heating will be presented, together with some other minor stress and temperature effects on NiTi modifying the hysteretic behavior.

Keywords: *diffusion, earthquake damping, finite element analysis, martensitic phase transformation, passive control, self-heating, shape memory alloys (SMA)*

Introduction

Increasing the quality of life is one of the main goals of smart materials and systems. In houses, one of the practical problems is the suppression/reduction of perturbation phenomena (vibrations/oscillations) via the integration of actuators and sensors in the structure [1]. In Civil Engineering two different kinds of oscillation phenomena can be considered. First, repeated or 'continuous' oscillations with different amplitude scales such as those induced by wind and rain in large structures (sky-scrapers, high towers and stayed cables in bridges). Second, the particular situation induced by earthquakes, scarce groups of large waves after several years of inactivity. This situation is different from other technical areas such as Mechanical Engineering where other time scales may be considered (for instance, groups of waves in relatively short time applications (i.e., one or two weeks) such as satellite launching or the continuous effects in the wheel-road interactions induced in driving cars.

The use of classical dampers, for instance, in reinforced isolated buildings (e.g. rubber-lead devices) requires re-centering devices and appropriate structure displacements permitting the bearings renewal after 10 or 20 years. The actual development of smart systems in damping for sky-scrapers, high towers and stayed cables in bridges uses tuned mass systems and/or dampers based in magneto-rheological fluids [2] with semi-active systems. These, and similar devices, need supervision and maintenance. For instance, the problems introduced by the eventual long time instability of the fluid, the intrinsic changes in hardware and software of computers modifying/affecting the proprietary programs need to be solved. In fact, all devices are inappropriate and expensive for relatively small constructions: at extremely long time (several decades) a well guaranteed passive method is a better approach.

In the recent literature, shape memory alloys (SMA) are suggested for damping in civil structures. The singular properties of the SMA i.e., the shape memory effect, the pseudoelasticity or the hysteresis cycle are due to a martensitic thermoelastic phase transformation between metastable phases. The SMA can be used as sensors and/or actuators and, also, their hysteresis cycle converting external work in heat allow the use of SMA as dampers (eventually working in martensite phase). In the passive application domain, without external power, the practical SMA can be classified in two groups, the Cu-based and the NiTi alloys. There are always possible some tunable actions (or use of semi-active control methods) for SMA, but the main interests in Civil Engineering time scales are their use as passive devices without continuous technical supervision or, eventually, the development of self-adjusting methods.

* Author for correspondence: vtorra@fa.upc.edu

1388–6150/$20.00

Akadémiai Kiadó, Budapest, Hungary
Springer, Dordrecht, The Netherlands

The use of SMA for earthquake damping requires a deep knowledge of static and dynamic properties of the alloy (i.e., the self-heating induced by fast cycling). Also, an evaluation of the long time diffusive contributions related to atomic order evolution is required. For instance, the devices need to be guaranteed after several decades of summer-winter temperature effects. Any evolution (macroscopic or microscopic) should be suppressed or, at least, controlled. The applicability of each alloy must be assured for each application. The successful applicability of NiTi in the health domain (i.e., orthodontic and surgical devices) [3] do not imply automatically an excellent behavior in other domains. Temperature changes of 40 K (i.e. summer–winter effect) in NiTi alloy always induces stress changes close to 240 MPa which represents near one third of the plastic deformation stress for this material after work or precipitation hardening.

The appropriate macroscopic and reproducible behavior of a SMA can be represented in the pseudo-elastic window or PEW (Fig. 1). The alloy works properly for stresses between $\sigma=0$ and $\sigma=\sigma_{pd}$, for deformations between $\varepsilon=0$ and $\varepsilon=\varepsilon_{max}$ and temperatures between T_2 and T_3. The PEW is experimentally determined by each thermo-mechanical heat treatment that ensures (or not) an appropriate material behavior. Damping earthquakes requires that the SMA remains inactive during decades before acting: it is necessary the study of the aging of SMA under the action of summer–winter temperature actions. Summer–winter temperatures act on the SMA behaviour via two complementary actions. The first is the macroscopic Clausius–Clapeyron coefficient. The action two is the aging at not constant temperature: a microscopic evolution induced by the yearly temperatures wave. Moreover, when the alloy works, the dissipated energy in the transformation between parent and martensite (latent heat and frictional contributions) changes the local temperature according the amplitude, the frequency of the oscillations and the type of alloy.

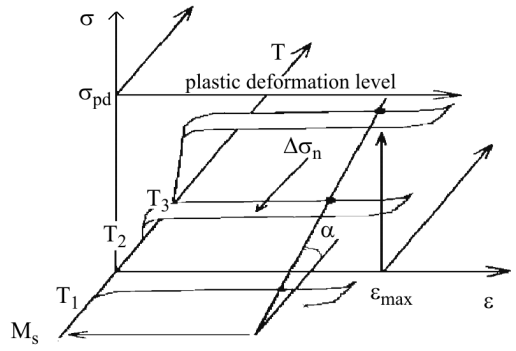

Fig. 1 Outline of the SMA behavior in σ, ε, *T* representation. Hysteresis width $\Delta\sigma_h$; σ_{pd} is the plastic stress boundary and the ε_{max} the maximal strain, the slope α relates the Clausius–Clapeyron coefficient ($d\sigma/dT$), the M_s is the martensite start temperature at zero stress

The present paper is the fourth of a series in SMA properties. In the first one [4] the time dependent and recoverable effects of thermodynamic forces (temperature and stress) on the CuAlZn single crystal was studied. Paper II [5] concerns the behavior of the CuAlBe polycrystalline SMA. It is focused on the thermo-mechanical treatments or sample preparation: homogenization in parent phase at high temperatures with increase of the grain size and, later, the appropriate long time aging at 373 K or at lower temperature. The main target of the heat treatment, aging, and so on relates a reduction of accumulative permanent deformation on cycling (or SMA creep). Paper III [6] was centered in some preliminary tests (more than one year of measurements) analyzing the time and temperature evolution of a NiTi alloy. In fact the NiTi is highly interesting alloy for working outside of buildings due to his resistance to external corrosion.

In this paper (paper IV) a scheme of the family house is outlined. The action is mainly centered on SMA dynamics for damping applications. In particular, the self-heating is studied. The particular parameters for CuAlBe are established and the stress and temperature effects in NiTi are, also, tentatively quantified. The house and a model of the SMA behavior are introduced in ANSYS visualizing the behavior of the structure under the action of an earthquake without and with SMA dampers [7].

An outline of the family house

Light buildings such as single or double-floor family houses under the effects of an earthquake of the literature (i.e. El Centro with magnitude 7.1 in the Richter scale) suffer oscillation amplitudes below 10 cm and reaction forces under 200 kN. These buildings are usually unprotected against earthquakes. To illustrate the damping capabilities of SMA, we have designed (Fig. 2) a building [8] according to Spanish structural standards [9]. The structure of the building has been designed with steel beams and concrete slabs to increase its robustness. Figure 2a shows a general view of the house. It is a two-storey building with near 200 m^2 on the ground floor and 100 m^2 on the first floor. The structure has two main sections divided by a ground garden. The back section has two floors and constitutes the main living area with an excellent sight over the garden situated in the roof of the front section. Figure 2b depicts the complete beam structure according to the structural requirements in

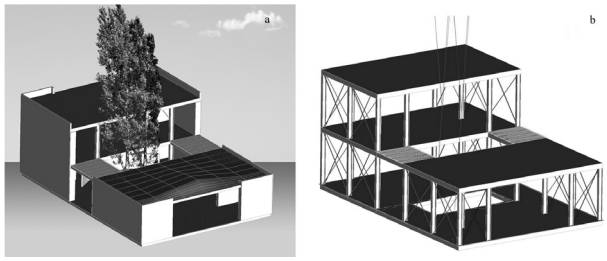

Fig. 2 a – External view of the sample family house. b – Structural sketch of the house showing the beam disposition and the possible emplacement for the SMA dampers on the portico diagonals

Barcelona. The possible emplacements for the dampers in the portico diagonals are, also, outlined.

In [7] an application to reduce the oscillation amplitudes by at least a factor 2 avoiding structural damage in the building is proposed. The system is passive and must not require constant supervision. The dampers are designed to work optimally for a given earthquake magnitude (for instance, near 7 in the Richter scale). For events below the nominal level neither the dampers nor the structure suffer any damage. Earthquakes in the nominal range produce damage in the dampers as they dissipate the mechanical energy. After the event it is necessary to revise the dampers. For larger earthquakes both the dampers and the building structure may suffer structural damage and must be checked afterwards. In this worst situation the dampers are still able to reduce the oscillation amplitudes by near a half.

Basic SMA behavior

The origin of the peculiar properties of SMA is a solid–solid phase transformation between two metastable phases. This thermo-elastic martensitic transformation produces a shape change (shear type) inducing, in single crystals, length change up to 10% in the appropriate crystallographic direction and, also, a hysteresis cycle (Fig. 1). Martensitic transformations may be induced by the thermomechanical actions (or thermodynamic forces) as stress (σ) and temperature (T). In the coexistence zone, the stress and the temperature are related by the Clausius–Clapeyron coefficient (CCC) ($\alpha=d\sigma/dT$). Figure 1 outlines the hysteresis cycles for different working temperatures. As the temperature increases, the stress to initiate the phase transformation also increases ($M_s<T_1<T_2<T_3$) according to thermodynamic formalism associated to CCC. The cycle is not modified by this shift but it is necessary to consider that working temperatures near the spontaneous transformation temperature (martensite start or M_s) may impede the return to parent phase in the unloading process due to the hysteresis width ($\Delta\sigma_h$) (for instance, the open cycle at T_1 in Fig. 1). Too high temperatures ($>T_3$) requires that the stress values overcome the plastic deformation level (σ_{pd}) for a given strain, producing a permanent deformation in the alloy. To use a SMA for damping in family houses it is necessary to determine the appropriate pseudo-elastic window (the PEW) ensuring the correct behavior of the damper when an earthquake occurs. In particular the length increases in cycling (or SMA creep) need to be avoided. It is also necessary to take into account the self-heating and the long time effects associated to diffusion phenomena.

In damping, the surface in the f–x (or σ, ε) representation (or the $\oint f\mathrm{d}x$) establishes the mechanical energy transformed in heat. The macroscopic thermo-elasticity or the slope ($d\sigma/d\varepsilon$) in the transformation zone, the hysteresis domain in coordinates stress (σ), deformation (ε) and temperature (T) and the Clausius–Clapeyron equation (relating the critical transformation stress with the room temperature) are the more relevant thermomechanical macroscopic properties characterizing the process. These properties depend on the materials characteristics, the sample preparation and, for instance, the self-heating of the sample while cycling (Fig. 3).

Studied alloys and experimental set up

In this work the applicability of two different SMA are studied. The first is CuAlBe, a Cu-based polycrystalline alloy. Wires of CuAlBe of several diameters were produced and furnished by Trefimetaux, France in the years 2003 and 2004. For the cast AH140 the reference data are: M_s=255 K; M_f=226 K; A_s=253 K; A_f=275 K with a chemical composition in mass%: Al=11.8; Be=0.5; Cu=87.7. The samples were cut, when necessary, by a low speed diamond saw (ISOMET), mechanically polished with fine grinding paper and, eventually, electropolished. The standard heat treatment for Cu-based alloys consists of an appropriate homogenization or betatization via a short time at high temperature (1123 K) followed by a fast quench in water at room temperature (293 K) and aging at 373 K for several hours. The second alloy is the NiTi. The analysis carried out in NiTi uses mostly wires with diameters of 0.5 'hard black oxide' and 2.46 mm 'light oxide' of superelastic Ni–Ti alloy from special metals [10] used 'as furnished' (55.8 mass% of Ni). In this situation, the grain size is around 50 nm from TEM analysis.

To characterize the behavior of SMA we have used four types of complementary experimental measurements.

- For thermomechanical and transient analysis (force or stress, deformation or strain, temperature and time), an INSTRON 5567 with cooler-heater chamber 3119-005 and a Materials Test System MTS 810 with home-made furnace, mainly for transient analysis. Also, equivalent home-made devices are used.
- For temperature induced transformation of aged NiTi the calorimetric equipment (model Q1000 DSC, TA Instruments [11]) and, also, resistance measurements provide information about the transformation temperatures at zero stress.
- The long time analysis is mostly measured using more than 4 figures in resistance measurements $R(t,T)$ and, for several days or weeks, the INSTRON 5567 and the ad hoc thermomechanical devices are used.
- Also, when necessary, X-rays and TEM or HRTEM are used to characterize the samples structure.

Relevant macroscopic SMA behavior (the Clausius–Clapeyron coefficient)

The relationship between stress-strain-temperature is determinant to establish the correct response of the dampers under the self-heating actions on working (Figs 3 and 4). The macroscopic effects induced by external temperature changes or by the self-heating during damping dissipation produce a displacement in the stress axis of the hysteresis cycle. A reasonable simulation requires a well known experimental value of the CCC $[(\mathrm{d}f/\mathrm{d}T)_{coex}$ or $(\mathrm{d}\sigma/\mathrm{d}T)_{coex}]$ with an uncertainty below 10%. The CCC can be well established for single crystals – in particular when parasitic effects as minor local composition changes and the intrinsic pseudoelasticity are minimized – from thermodynamic analysis in the frame of the first and second thermodynamic laws [12, 13]. However, in polycrystalline materials the progressive interaction among martensite variants provides a cycle with high macroscopic pseudoelasticity (relevant slope in the transformation zone in Fig. 4b) and it is necessary to experimentally evaluate the CCC for each wire type (Table 1). In the CuAlBe alloys the starting part of the transformation (deformation under 2 or 3%) is used in order to avoid the accumulative creep. In NiTi, it is convenient to do some preliminary cycles, the inflexion point in the transformation path ($\partial^2 f/\partial x^2=\partial\sigma^2/\partial\varepsilon^2=0$) is used to evaluate the CCC. For a series of cycles the hysteresis cycle approaches the asymptotic shape of Fig. 6. After several sets of measurements, the CCC for CuAlBe is close to 2.2 MPa K^{-1} and, for NiTi, the value approaches 6.3 MPa K^{-1}. The overall uncertainty is situated below 10%.

Cycling effects: self-heating and SMA permanent deformation

In the transformation and retransformation process the self-heating relates the latent heat released and absorbed by the specimen, and the hysteretic contributions making a transformation of mechanical work in dissipated heat. For instance, the irreversibility increases with the parasitic effects (dependent of the cycling rate and sample characteristics) induced by the heat transmission to and from the surroundings. These effects are highly dependent on the frequency rate, deformation percent and sample cross section as shown in Fig. 3. At the present state of the art, each alloy wire requires an independent evaluation.

Using a thermocouple attached to the sample the temperature evolution can be followed. Figure 3a shows the thermal effects related with cycling frequency for a CuAlBe wire of 3.4 mm. In the experiments, oscillations with amplitude up to 3.5% can produce average temperature fluctuations over 10 K for frequencies of 1 Hz. If we compare the increase of temperature in samples due to cycling for a frequency of 0.25 Hz in NiTi and in CuAlBe, we can see that the effect of self-heating is much higher in NiTi. Figure 3b shows some asymptotic values for NiTi wires with a diameter of 2.46 mm. In the study of the dynamic behavior in NiTi it seems that the experimental temperature increase is approximately three times to that observed in equivalent CuAlBe samples. The higher value of CCC in NiTi produces a progressive increase of transformation stresses, due to the self-heating in a 'fast' cycling at 0.5 Hz (Fig. 4).

The application of the material for damping the oscillations induced by external actions in structures requires that the cycles do not produce progressive permanent deformation. In CuAlBe, the accumulative deformation is produced by plastic deformation and, also, by partial martensite stabilization. In the NiTi more analysis seems necessary. If the material in-

Table 1 Experimental CCC values for the studied CuAlBe and NiTi alloys (SM=special metals)

Sample	CuAlBe (NIMESIS)	CuAlBe (Trefimetaux)	NiTi (SM)	NiTi (SM)
CCC/MPa K^{-1}	2.12	2.26	6.23; 6.59	6.38; 5.94
Diameter/mm	1.6	3.4	0.5	2.46
Cycles studied	1 to 3	1 to 3	1 and 130	1 and 130

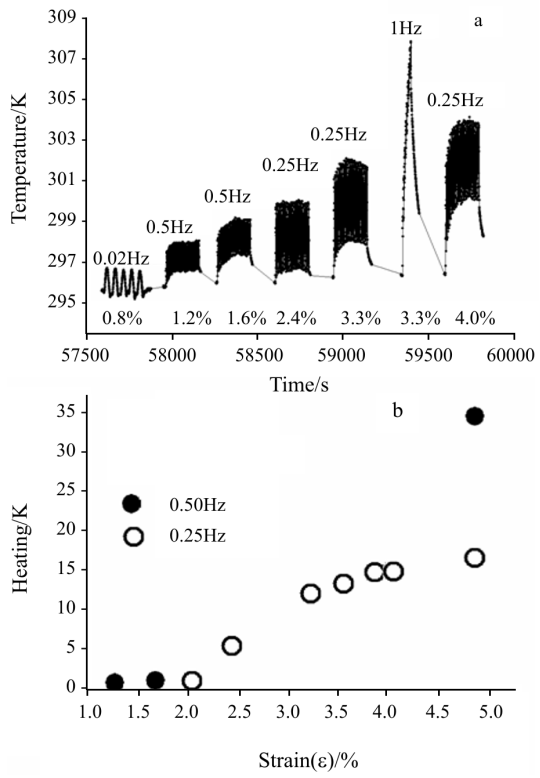

Fig. 3 a – CuAlBe alloy (130705) (diameter=3.4 nm). Temperature evolution on cycling for different amplitudes and frequencies. b – Tentative temperature increase in steady state for NiTi (diameter=2.46 nm) *vs.* the deformation per cent for cycling frequencies 0.25 and 0.5 Hz

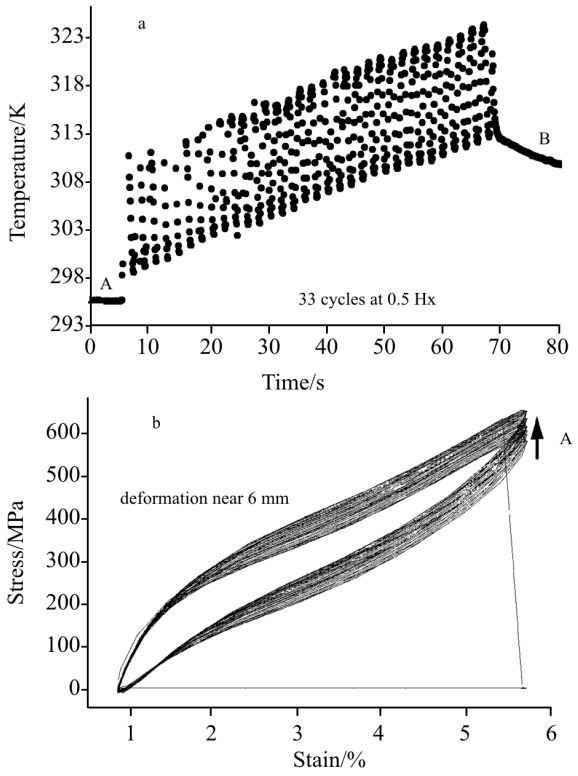

Fig. 4 a – Dynamic of the self-heating effects in NiTi wire (1207ND6) (diameter 2.46 mm) for 5% of deformation at 0.5 Hz; A – initial wire temperature; B – spontaneous cooling after the fracture of the wire. b – Increase of the stress close to 100 MPa (arrow A) with cycling, NiTi (1207ND6), (diameter 2.46 nm)

creases progressively and permanently its length, the net strain produced by the structure oscillations during the earthquake is reduced. If such deformation is large enough the alloy may not even start the transformation and not energy dissipation is possible. The preparation of SMA is crucial for keeping creep at zero or in acceptable values and avoiding the modification of the hysteresis cycle.

In the case of CuAlBe, the classical heat treatment for CuAlBe samples with a 3.4 mm diameter, consists in the standard betatization of the alloy, i.e., two minutes at 1123 K with immediate quenching in water and, later, 1 h at 373 K, provides a wire with a satisfactory level of working stresses (fracture above 350 MPa) and deformation (6% or more) for a series of cycles. The material in these conditions shows the relevant and accumulative permanent deformation (SMA creep) while cycling. The available working deformation is nearly constant at 3% as an increasing creep tracks the progressive deformation (Fig. 8 in paper II [5]).

Some thermomechanical development for CuAlBe is established that permits to nearly eliminate the creep inside the PEW. By increasing the homogenization (or betatization) time we increase the grain diameter (i.e., the mean grain radius roughly changes from 0.14 to 0.75 mm), 'approaching' the behavior of a single crystal. The extended time in the furnace at 1123 K, the lengthy aging at 373 K and subsequently a thermo-mechanical treatment reduces the accumulated deformation for deformations under 5% with minor degradation of mechanical properties (fracture level remains close to 250 MPa). The observations recommend using a deformation under 4.5% (maximal available under 6%) with a remnant deformation below 0.5% and associated stress close to 250 MPa at room temperature (293 K), as can be seen in Figs 5a and b. The sample fracture appears around a maximal deformation of close to 6%.

In the case of NiTi the creep of a NiTi sample with a standard heat treatment is strong, as it can be seen in Fig. 6. In this case the stress overcomes 700 MPa and the sample is plastically deformed. The cumulative creep and the cycle deformation with a great loss of hysteresis width are clearly observed. At the present state of the art an efficient treatment for NiTi, as established for CuAlBe, is not available.

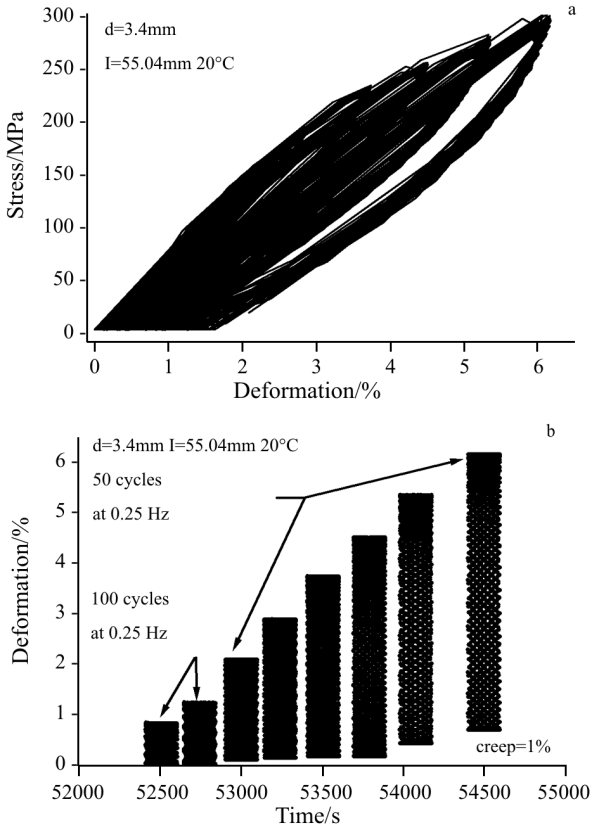

Fig. 5 a – Hysteresis cycles for progressive deformation. The device apparently suppresses the effects of progressive deformation via free behavior in the compressive part. b – Reduction of remnant deformation in CuAlBe samples with larger grain diameter and longer aging

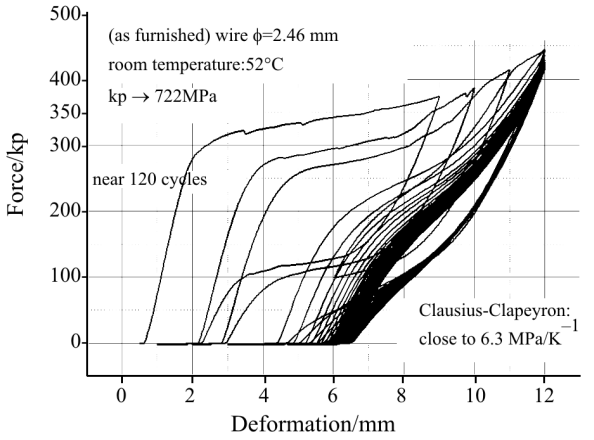

Fig. 6 Hysteretic behavior for NiTi alloy at 325 K. Progressive creep on cycling

Diffusion effects in CuAlBe

On the other hand, the metastability of the phases induces microscopic changes in atomic order. Long time effects can be observed in samples aging. Figure 7 shows the experimental analysis of the variation of M_s as a function of the time elapsed after the quenching procedure for a CuAlBe alloy. Two temperatures and times were used: 100 days at 373 K and, 150 days at 353 K. After 250 days of M_s evolution in aging, the M_s slowly tracks the 'room temperature' evolutions (i.e., for steps of 50 days at constant temperature). For instance, the change in M_s value associated to changes of 20 K in the external temperature is close to 4 K (near 20%). It suggests that the summer–winter effect in CuAlBe alloy under temperature changes of 40 K can produce M_s evolutions near 8 K. The effects, under the action of room temperature, are smoothed by the higher value of the associated time constants. After aging, the M_s can be predicted as a function of the room temperature using Eqs (1) and (2) established in paper I [4].

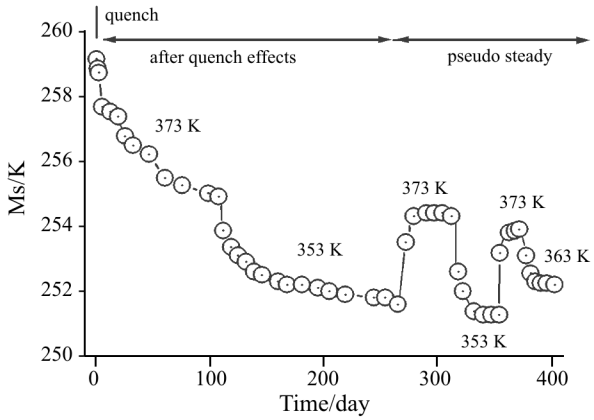

Fig. 7 CuAlBe: the after quench M_s changes with aging at different temperatures

Parent and martensite phases coexist along the whole transformation curve. The static or the dynamic coexistence, when cycling, produces changes related to diffusion (enhanced by the presence and displacement of interfaces) and to self-heating produced by the frictional contributions associated to the hysteresis cycle. In Cu-based and 'quasistatic' conditions, a progressive increase in the quantity of martensite is observed at constant stress and temperature [4, 15]. Also, at constant strain, a decrease of stress would exist. In dynamic conditions, the experimental results show two opposite behavior. The self-heating associated to fast cycling would produce an increase of the maximum force of the cycle (as shown in Fig. 4). On the other hand, in CuAlBe, the measurements suggest that the transformation temperature evolution due to coexistence is opposite to the self-heating effect: Maximum stress might reduce slightly for thin wire at low frequencies (Fig. 8). However, the dynamic coexistence effects in cycling can be masked by the self-heating.

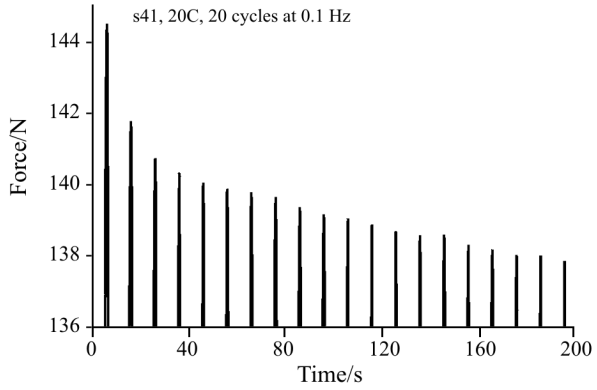

Fig. 8 Progressive decrease of maximal force in a series of hysteresis cycles for CuAlBe alloy. Slow cycling at 0.1 Hz with a wire of CuAlBe alloy (diameter close to 1 mm). The stress reduction is close to 5 MPa or, via the CCC, 2.5 K

Diffusion effects in NiTi

The experimental analysis of the diffusion effects in NiTi is only in the preliminary steps after 1.5 years of measurements. The dynamic effects are extremely slow and require relative higher resolution and measurement time. The measurements are centered in four aspects: stress in parent phase, in phase coexistence and in martensite and temperature effects on aging. The effect of the aging temperature is an evaluation of the direct sun effect on the NiTi wires/bars situated, for instance in the roof of the buildings. The diameter of used wires is 0.5 mm.

Loading effects in parent phase

We have made experiments holding the NiTi wire at a fixed strain during near 1 month and then continuing the cycle. We repeated the experiment stopping at different points of the load part (Figs 9a–c). Firstly we studied the effect of stopping at different points when the applied force corresponds to a strains situated in

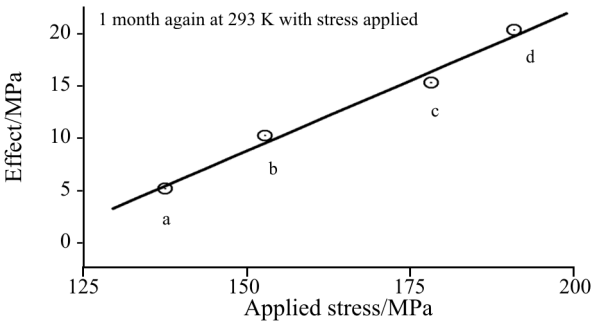

Fig. 9 Stress changes related to the applied stress at 293 K. One month aging at 293 K with stress applied at different points of the elastic zone (points a, b and c) and d point in the coexistence zone

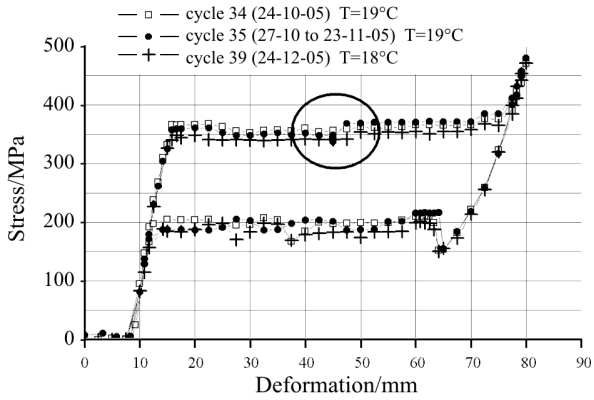

Fig. 10 Hysteresis cycle for NiTi wire of 0.5 mm of diameter. Effect of 27 days aging with stress applied in coexistence zone at near 292 K

the elastic zone of the hysteresis cycle. The point d is obtained from the coexistence zone. We obtained that the higher the holding stress the greater the residual cycle is displaced to higher stresses. The evaluation of this effect at room temperature can be observed in Fig. 9. The increase of the stress is, roughly, proportional to the previous stress ($100\Delta\sigma/\sigma=27\%$).

Loading effects in coexistence

When the applied force is hold at the coexistence zone, as it can be seen in Fig. 10, a step appears in the hysteresis cycle. The global increase of the stress to be able to continue the cycle after one month reaches the 35 MPa, corresponding to an increase in parent and a decrease in martensite phase.

Loading effects in martensite

In martensite, the 'stress-aging' study was performed at different times. We hold the strain at the end of the transformation with the 'same' applied stress for different times continuing then with an inner loop as shown in Fig. 11a. The experimental observations establishes that the longer the time hold in complete martensite state, the lower the stress to re-start the transformation in the inner loop and, consequently, the observed step is higher. Figure 11b shows the step dependence with the aging time near 293 K.

Temperature effects

The preliminary observations of the temperature aging effects at 373 K were presented in paper III [6]. Afterwards, the analysis was continued for 150 additional days with more samples and, also, with the results associated to aging at 338 K (Fig. 12). The results at 373 K indicate that the time constant is close to 250 days and the asymptotic value of M_s (or R_s, par-

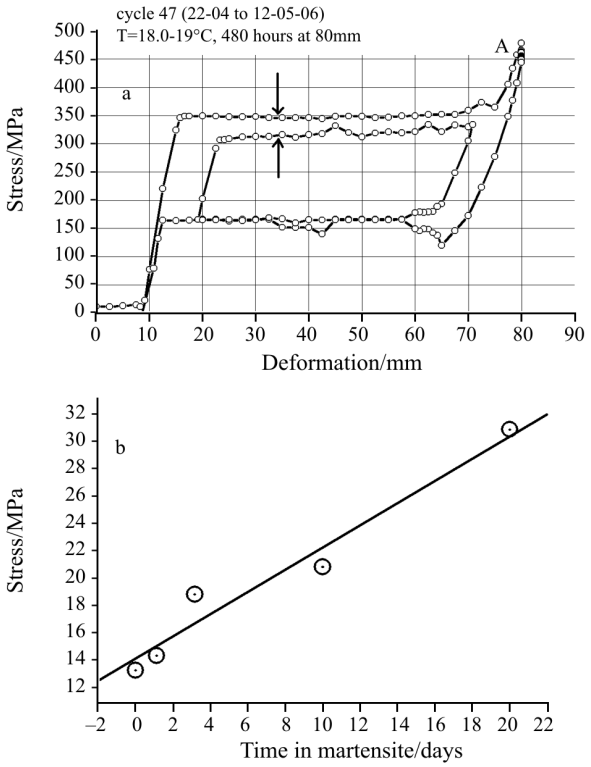

Fig. 11 Effect of aging at 293 K with stress applied when all is transformed to martensite (position A). a – hysteresis cycle with an inner loop after the aging. b – step values *vs.* aging time in martensite

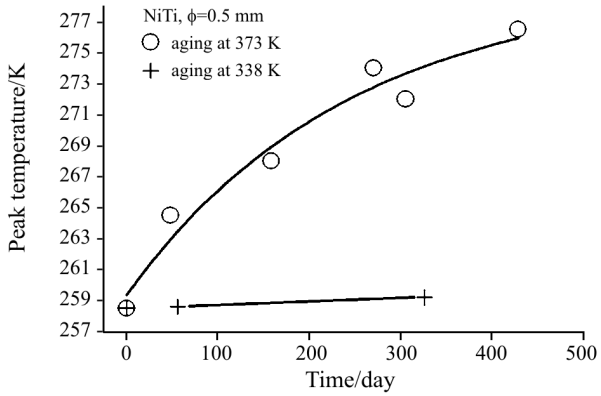

Fig. 12 Transformation peaks *vs.* the aging time in days at temperatures ○ – 373 K and + – 338 K

ent-martensite transformation) change around 20 K. For 300 days at 338 K the time constant is extremely higher and the asymptotic value unavailable. The complete calorimetric measurement (paper III [6]) suggests that the M_s decreases evolving in opposite way compared to the R_s, that increases. Complementary measurements of structural evolution with temperature are necessary.

The experimental analysis at this preliminary level suggests that the use of NiTi for several years in pre-stressed devices and, also, their uses in outside areas, under direct sun actions, can produce unexpected behavior changes. Quantifying these changes requires several years of measurements as indicates, for instance, the time-scale of Fig. 12. In other words, despite NiTi is good for outside applications, due to the resistance to the weather and environmental changes, the use for several years can not be guaranteed with the actual level of knowledge about the diffusion time scale effects.

SMA behavior

A phenomenological approach suggests that the temperature and the stress in parent phase produce a similar effect [4, 14]. The internal state of the sample under the external thermodynamic forces is progressively modified. The analysis via external temperature actions in parent phase (Table 2) shows that the transformation temperature tracks the external temperature via an exponential behavior [15]. Each time constant, highly temperature dependent, is related to some activation energy. Table 2 shows the transformation temperature changes associated to a step at room temperature (close to 10% for one time constant), the time constant and the activation energy for CuZnAl (for CuAlBe only one activation energy is evaluated) and an approach to the values for NiTi. Ex-

Table 2 Diffusion phenomena and asymptotic temperature effects on M_s for the studied alloys

Alloy	CuAlZn [15]	CuAlBe	NiTi
τ_1 at T	1390 s at 373 K	1.95 days at 373 K	1.9 days at 410 K
τ_1 at T	11020 s at 353 K	4.63 days at 353 K	55 days at 363 K
Activation energy	13630 K	5790 K	10700 K
τ_2 at T	47200 s at 373 K	–	–
τ_2 at T	226700 s at 353 K	–	–
Activation energy	1030 K	–	–
$100\Delta M_s/\Delta T_{RT}$	$-(10.5_{(1)}+6.7_{(2)})$	$14_{(1)}$*	$15_{(1)}$**

*only one time constant from M_s measurements. **rough approach, time constants are from resistance measurements *vs.* time; M_s (or R_s) changes are determined from changes on peak positions in DSC measurements

trapolation of NiTi time constant values at human body temperatures gives more than 100 years; and due to the moderate amplitude of the changes, the effects are non-relevant for most room-temperature applications. In Civil Engineering, for elements that can be exposed to outdoor conditions or to sunlight, some considerations are needed.

All these physical properties of SMA can be summarized in the definition of the PEW. The contribution of each effect is evaluated as a temperature increase, which can be converted in a stress change through the CC coefficient. The PEW must consider all relevant effects plus a certain security level. Table 3 shows the evaluation of the PEW for the studied alloys. From these results the importance of CCC is shown.

Table 3 Expected changes in CuAlBe and in NiTi alloy. The CCC approaches respectively 2.2 and 6.3 MPa K^{-1}. The manufacturer establishes that the yield strength in NiTi is close to 800 MPa

Parameter	ΔT/K (CuAlBe)	ΔT/K (NiTi)
Hysteresis width	30 to 50	15 to 35
Summer–winter	40	40
Self-heating (3.5%)	10	20
After quenched sample	5	–
Phase coexistence (dynamic)	–10	–4.5*
Summer–winter tracking and asymptotic	3; 5.5	1; 6*
Security level	10 to 20	10 to 20
Global effect	110 or near 240 MPa	100 or near 630 MPa

*indicative values

Damper design

A SMA damper may be simply a wire of material that due to its hysteresis cycle is able to convert mechanical energy into heat. In principle we may use a single SMA rod with a sufficient thickness to endure the stress (traction and compression) in the structure. However there are several reasons that suggest the use of a set of thinner SMA wires instead. Firstly, to be able to use the material it is necessary to prepare the sample with a thermomechanical treatment ('Cycling effects: self-heating and SMA permanent deformation'). This sample preparation loss its efficiency with the thickness of the sample: the sample thickness by the Fourier heat transfer equation imposes a temperature gradient in the betatization process that prevents appropriate M_s homogenization. Secondly, the grain complexity grows with the sample thickness. This produces the increase of undesired material behavior which modify the hysteresis shape. For these reasons we propose a damper structure with N thin wires (diameter less than 5 mm) as depicted in Fig. 13. Obviously this configuration only allows the dampers to work in traction. No compression work is possible. To solve this limitation the dampers always work in pairs on a counteracted geometry.

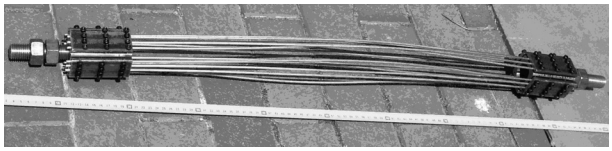

Fig. 13 Picture of an experimental SMA damper built from 12CuAlBe wires of diameter 3.4 mm

The detailed properties of a wire depend on the composition, the sample preparation and the thickness. The design and optimization of the dampers consist on determining the best length and number of wires that compose each damper. We are using CuAlBe wires of diameter 3.4 mm able to undergo a stress of 2.5 kN with an ultimate strain of 5% without relevant 'SMA creep' on working. To ensure an appropriate response of the dampers we consider strains up to 4%. This limitation has two reasons: to reduce the accumulated creep and to provide a safety margin. The calculation of the maximum strain and stress for each damper requires the analysis of the structure under the effects of an earthquake. By studying the free oscillation of the building we obtain the free oscillation amplitude (avoiding any plastic deformation of steel), the stresses induced in the structure and, from the steel plastic deformation level, the maximum deformation that the structure can undergo without plastic deformation. From the free oscillation amplitude we determine the length of the SMA wires in order to not overcome the maximum strain (do not enter inside the steel plastic deformation). We calculate the number of wires required to produce a total stress around 10–30% of stresses induced in the structure by the event. Usually, starting from this calculated data, an iterative process is required to fully optimize the dampers.

SMA model for structural simulations

Modeling the SMA behavior is a complex topic of permanent interest. See for instance [15] and related references and, for several recent approaches [16–20]. The inherent complexity of the martensitic transformation of SMA requires a formulation at various depth levels. The importance of each level depends on the requirements to be satisfied by the material in the working situations. Each material presents several different time scales. There are fast effects re-

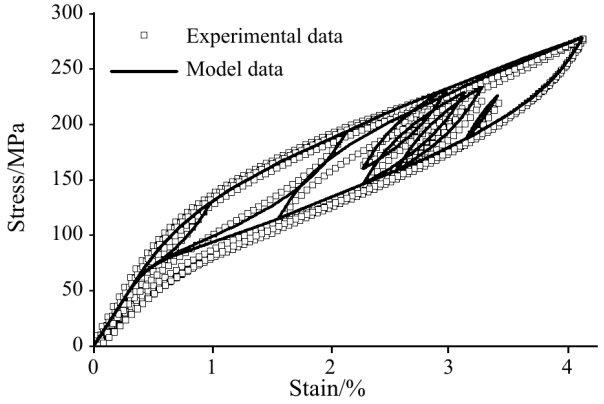

Fig. 14 Experimental and simulated behavior of a CuAlBe sample

lated with thermomechanical oscillations governing the damping actions under earthquake effects and slow effects governed by atomic diffusion that determine the material lifetime. All these effects should be considered when dealing with damping applications for long lifetime. So far a detailed unified treatment of the 3-D systems (including traction-compression-bending) is, still, a research topic. We have developed a simplified 1-D model with physical image appropriate for damping applications in civil engineering. This model is developed for polycrystalline CuAlBe alloys where the single element model (the bilinear model) is insufficient for internal loops, i.e., improving the agreement between the model and the experimental loops is needed. This model is composed by a set of parallel transformation domains. The parallel configuration is suited for simulation environments where elongation is the element input parameter such as ANSYS [21]. Besides, this structure is particularly valid for polycrystalline alloys as has been reported for similar materials [22]. This model is composed by 9 parallel elements. Figure 14 shows the model and the experimental data for CuAlBe. The model accuracy for global, partial and internal cycles is very good with a computation time similar to the single bilinear model.

We focus on the single floor section of the family house of Fig. 2, with the elevated garden (Fig. 15a depicts the beam structure and damper positions). As the structure we consider is composed by a set of three triple porticos we analyze here only the triple portico (central) with highest load. This simplifies the design process. Figure 15b sketches the three-arch portico with its load and characteristics. The portico height is 3 m. The width of the arches is 2.35 m (lateral) and 6.80 m (central). The pillars are build by HEB200 beams (central columns) and HEB140 (external pillars). The horizontal girders are HEB240 for the central arch and IPN160 for the lateral ones. The total portico load is $46.5 \cdot 10^3$ kg. The pairs of dampers are installed in the diagonals of the

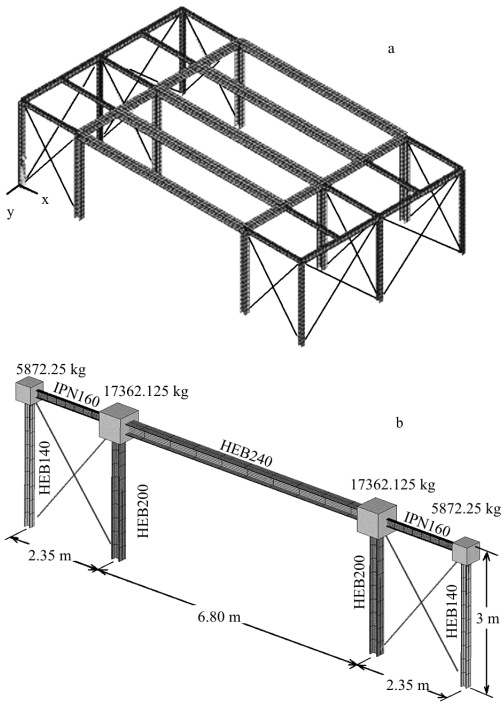

Fig. 15 a – Beam structure for the garden section with the placement of SMA dampers. b – Schematic description of the garden central triple portico with H (vertical) and I (horizontal) steel elements, the loads and the SMA damper situation

lateral arches permitting free displacements for the center of the chamber. Steel cables (with higher stiffness than the dampers) are used to link the dampers with structure permitting zero stress in compression parts of the oscillations.

Using the structural software ANSYS in which our models has been included by a proprietary USERMAT routine, we analyze the response of the portico under the action of an earthquake. Several earthquakes has been used, but the most detailed analysis and the optimization of the dampers has been performed using the data from 'El Centro' seism [23] (1940) with magnitude 7.1 (Richter scale). Figure 16a shows the acceleration pattern for this seism. It produces a horizontal oscillation on the upper section of the portico of amplitude 7.3 cm (Fig. 16b) and the reaction forces involved are close to 650 kN with a maximum absorbed energy of 23.4 kJ.

We have designed the dampers using CuAlBe wires with diameter of 3.4 mm. After some iterative analysis the best results are obtained using a set of 25 wires with length 0.6 m that reduces the maximum oscillation amplitude to 3.2 cm. The damper dissipates 66% of the energy transmitted to the structure. Figure 16c shows the oscillation amplitude of the response of the portico to 'El Centro' using CuAlBe dampers. The expected quantity of CuAlBe is close to 4.8 kg.

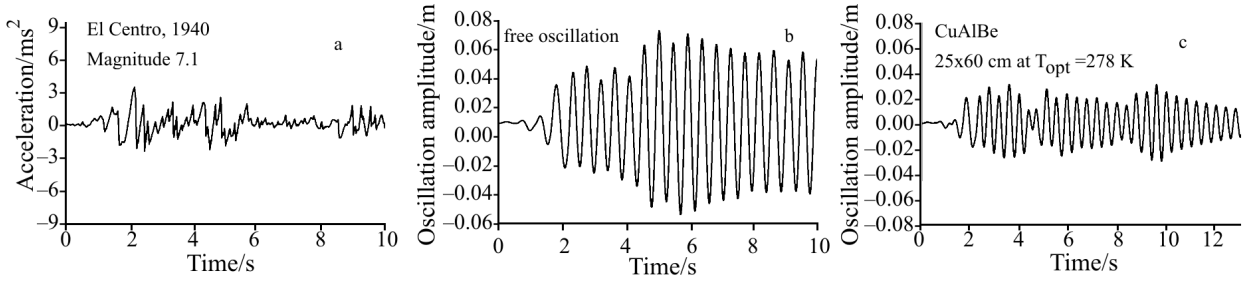

Fig. 16 a – Acceleration pattern for 'El Centro' earthquake (magnitude 7.1 in the Richter scale); b – oscillations induced in the portico (linear steel model) without dampers; c – detailed response of the portico to 'El Centro' using SMA CuAlBe dampers

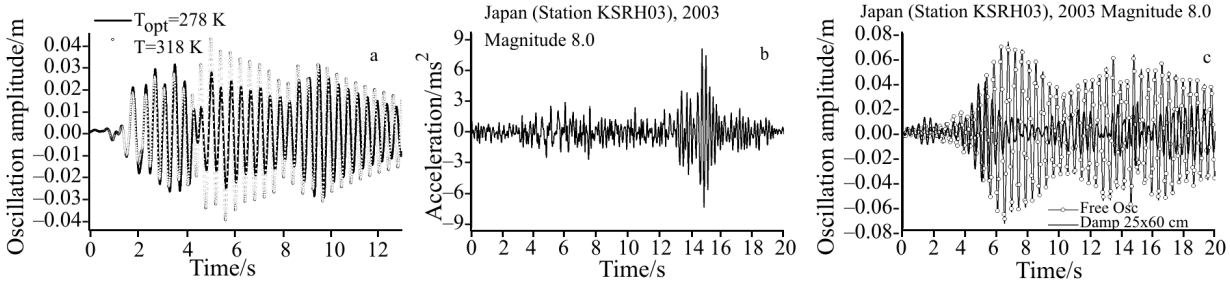

Fig. 17 a – Portico response with SMA dampers at different temperatures. Optimal temperature (T_{opt}, line) and worst case simulation (T=T_{opt}+40 K, dots) for CuAlBe; b – acceleration pattern for the Japan earthquake (magnitude 8.0 in Richter scale) recorded in station KSRH03 in 2003; c – simulated oscillations induced in the portico without dampers (line plus dots) and response of the portico using SMA CuAlBe dampers (line) for the same earthquake

It is important to evaluate the material behavior under extreme conditions. To perform this simulation we increase the working temperature. The temperature increase must consider the external temperature fluctuations (summer–winter), the material self-heating, the atomic diffusion effects and a certain security margin according to 'SMA deviation'. We have evaluated this temperature increase as 40 K. Figure 17a compares the damper response in the optimal conditions (T_{opt}, line) and under worst case conditions (T_{opt}+40 K, dots) for El Centro earthquake. The results demonstrate that the dampers are robust and able to work even in this extreme situation. The maximum oscillation is higher but the damping is still important (3.1 cm in nominal in front of 4.2 cm in worst conditions against 7.3 cm without dampers).

Once the dampers are optimized for a particular earthquake it is necessary to check whether they are valid for other events as each earthquake seismogram contains its own frequencies that combined with the building 'resonant frequencies' (non-linear behavior) can produce very different effects. We have simulated the triple portico response for different recent Japanese earthquakes. One example is the registered in the station KSRH03 of magnitude 8.0 [24] Richter scale, in Japan, 2003. Figure 17b presents the accelerogram for the event, and in Fig. 17c the free oscillation (line plus dots) and the damped oscillation with the designed SMA dampers with CuAlBe (line) are shown. Also the oscillation amplitude with the SMA dampers is reduced to a half of the expected amplitude without dampers.

Conclusions

SMA alloys are suitable materials for the development of solid-state dampers in Civil Engineering. Dampers with forces near 60 kN can be built from several wires of SMA with total cross sections around 300 mm^2 of CuAlBe with an acceptable working strain close to 3.5–4.0% (maximum deformation near 5%). Using these dampers we have designed a damping system for a family house which is able to reduce the maximum oscillation amplitudes induced by high magnitude earthquakes by approximately a factor 2 and dissipating nearly a 50% of the energy adsorbed by the structure. The paper describes the SMA appropriate properties for the dampers and analyzes the extreme working conditions (in temperature, maximum displacements and material aging) using ANSYS structural simulations.

Several years of observations in CuZnAl, CuAlBe and, partially, NiTi suggest that the studied alloys show similar behavior with different time scales (1:4:250). These observations provide the required knowledge to guarantee the material behavior for long time applications (several years) under the action of the summer–winter temperature actions and

atomic diffusion effects. Accurate time-analysis determines the time scales and the changes on the hysteresis cycle.

A thermal and thermomechanical treatment is developed for CuAlBe. The use of improved Cu–Al–Be wires permits near 4.5% of deformation without progressive permanent deformation (the SMA 'creep') on cycling. The phenomenological behavior (and the internal loops) can be modeled using a 1-D parallel model. Simulation in ANSYS shows that the dampers reduce the oscillation amplitude to a half. The partial analysis of the diffusion contributions in NiTi shows extremely larger time scales. At the present state of the art, the use of NiTi dampers in direct sunny actions or in pre-stressed condition for several years or decades seems dangerous. More studies about the evolution of the NiTi properties with time is necessary.

Acknowledgements

Work realized in the frame of Spanish projects: MAT2002-10423E (MEC), PCI2005-A7-0254 (MEC) and FPA2000-2635-E (M.F.). The NiTi analysis remains under the ESF EUROCORES S3T project number 05-S3T-FP014-SMARTeR. Cooperation between CIRG (UPC) and with CAB-IB (University of Cuyo, Argentina) is supported by CNEA and, in the past, by DURSI (Gen. Catalonia). V. T. acknowledges support in NiTi analysis from Dr. A. Yawny and Eng. H. Soul. Experimental support from Mr. Pablo Riquelme and creative ideas in the development of hand controlled devices from Mr. Raul Stuke are acknowledged. Calorimetric measurements are realized by Mr. Sergi Ruiz in TA Instruments, Cerdanyola (Barcelona).

References

1 Adaptronics and Smart Structures, H. Janocha, Ed., Springer (1999).
2 http://www.lord.com.
3 K. Otsuka and C. M. Wayman, Eds, Shape Memory Materials, Cambridge University Press, Cambridge 1998.
4 V. Torra, J. L. Pelegrina, A. Isalgué and F. C. Lovey, J. Therm. Anal. Cal., 81 (2005) 131.
5 A. Sepúlveda, R. Muńoz, F. C. Lovey, C. Auguet, A. Isalgué and V. Torra, J. Therm. Anal. Cal., OnlineFirst, DOI: 10.1007/S10973-005-7480-3.
6 C. Auguet, A. Isalgué, F. C. Lovey, J. L. Pelegrina, S. Ruíz and V. Torra, J. Therm. Anal. Cal., OnlineFirst, DOI: 10.1007/s10973-006-7625-z.
7 V. Torra, A. Isalgué, F. Martorell, P. Terriault and F. C. Lovey, Eng. Struct., DOI: 10.1016/j.engstruct.2006.08.28.
8 Family house designed by R. M. Torra, Arch. (rmtorra@coac.es).
9 Structure (beams and pillars) calculated according to the Barcelona norms, by A. Vera, Arch. (averagq@coac.net).
10 http://www.specialmetals.com.
11 http://www.tainst.com.
12 P. Wollants, J. R. Roos and L. Delaey, Prog. Mater. Sci., 37 (1993) 227.
13 V. Torra, Shape Memory Alloys: Fundamentals, Modeling and Applications, V. Brailowski, S. Prokoshkin, P. Terriault and F. Trochu, Eds, Ecole de technologie supérieure, Montreal, Canada 2003, p. 9.
14 J. L. Pelegrina and M. Ahlers, Scripta Mater., 50 (2004) 423.
15 F. C. Lovey and V. Torra, Prog. Mater. Sci., 44 (1999) 189.
16 R. DesRoches, R. T. Leon and J. Ocel, Proceedings of 3rd World Conference on Structural Control, Como, Italy 2002, Vol. 2, p. 375.
17 L. Faravelli, Proceedings of 3rd World Conference on Structural Control, Como, Italy 2002, Vol. 2, p. 163.
18 M. Collet, E. Foltete and C. Lexcellent, Proceedings of 3rd World Conference on Structural Control, Como, Italy 2002, Vol. 2, p. 174.
19 P. Terriault, V. Brailowski and K. Settouane, Proceedings of 3rd World Conference on Structural Control, Como, Italy 2002, Vol. 2, p. 369.
20 F. Martorell, A. Isalgue, F. C. Lovey, A. Yawny and V. Torra, SPIE'04 Sidney, Australia 2004, Smart Materials 3, Proceedings of SPIE, Vol. 5648, p. 194.
21 http://www.ansys.com.
22 Y. Sutou, T. Omori, K. Yamauchi, N. Ono, R. Kainuma and K. Ishida, Acta Mater., 53 (2005) 4121.
23 http://nsmp.wr.usgs.gov.
24 http://www.kyoshin.bosai.go.jp/k-net/search/index_en.html.

DOI: 10.1007/s10973-006-8034-z